Available online at www.sciencedirect.com

ScienceDirect

Scripta Materialia 69 (2013) 630–633

Scripta MATERIALIA

www.elsevier.com/locate/scriptamat

Solute redistribution in the nanocrystalline structure formed in bearing steels

J.-H. Kang,[a] B. Hosseinkhani,[b] C.A. Williams,[c] M.P. Moody,[c] P.A.J. Bagot[c] and P.E.J. Rivera-Díaz-del-Castillo[a,*]

[a] *SKF University Technology Centre, Department of Materials Science and Metallurgy, University of Cambridge, Cambridge CB2 3QZ, United Kingdom*

[b] *Department of Lubrication and Metallic Materials, SKF Engineering and Research Centre, Kelvinbaan 16, 3439 MT Nieuwegein, The Netherlands*

[c] *Department of Materials, University of Oxford, Oxford OX1 3PH, United Kingdom*

Received 19 June 2013; revised 4 July 2013; accepted 16 July 2013
Available online 24 July 2013

The microstructural alteration in a white etching area (WEA) formed during rolling contact fatigue of a 1C–1.8Cr steel (wt.%) is studied. A uniform nanocrystalline structure with scattered carbide particles is observed. Si and C atoms segregate to different regions in the cell boundaries, implying a repelling behaviour. Carbon-rich clusters were identified but contained less than 25 at.%C. It is suggested that the interaction between Si and C should be considered in the mechanism for microstructural decay.

Keywords: Fatigue; Transmission electron microscopy (TEM); Atom probe tomography; Martensitic steels; Deformation structure

The effective life of bearings is determined by rolling contact fatigue (RCF) due to repetitive contact between the elements during their operation [1]. When a material fails by RCF after a long operation period, spalling occurs as a result of cracks initiated and propagated from the subsurface where microstructural alteration is observed [1,2]. Among the forms of microstructural damage, the formation of white etching areas (WEAs) is closely related to cracking, since such areas are attributed to the stress concentration adjacent to cracks [3]. Most academic studies on WEAs deal with "butterflies", formation of which is associated with inclusions around which nanocrystalline structures and carbide dissolution are observed [4–6]. The scale of the nanocrystalline structure varies with the distance from the inclusion. Some authors claim complete carbide dissolution in the WEA [6], while others report fine (~7 nm) carbides within it [4,5].

The formation of WEAs due to large stress concentrations is comparable to other processes that result in similar microstructural alterations. Examples include severe plastic deformation (SPD) during wire drawing [7], mechanical milling [8], high pressure torsion [9], surface mechanical attrition treatment [10], and ball drop testing [11] of pearlitic steels. The white etching layer (WEL) observed in pearlitic rail steels is of a similar nature [12]. This implies that the stress concentration adjacent to the cracks in bearing steels is as extreme as in SPD. With the aid of advanced characterisation techniques such as transmission electron microscopy (TEM) [7,8,11,10], atom probe tomography (APT) and field ion microscopy [7,8], Mössbauer spectroscopy [13], and synchrotron X-ray diffraction [14], not only nanocrystalline structure and carbide dissolution, but also carbon segregation to crystalline defects has been revealed for SPD.

In this study, TEM and APT were employed to investigate (i) the similarities between WEA and SPD microstructural changes, (ii) the presence of carbides in WEAs, and (iii) the distribution of alloying elements in the WEA. Based on these results, mechanisms of microstructural alteration in WEAs are suggested.

The sample is a RCF-tested 100CrMo7 bearing steel: 0.970 C-1.80 Cr-0.325 Si-0.325 Mn-0.020 Mo-0.25 (max.) Ni-0.25 (max.) Cu–Fe (wt.%). The sample was partially austenitised at 830–870 °C, quenched in salt bath, and tempered at 230–250 °C. The resulting microstructure before testing assumes tempered martensite

* Corresponding author. Tel.: +44 1223334700; e-mail: pejr2@cam.ac.uk

1359-6462/$ - see front matter © 2013 Acta Materialia Inc. Published by Elsevier Ltd. All rights reserved.
http://dx.doi.org/10.1016/j.scriptamat.2013.07.017

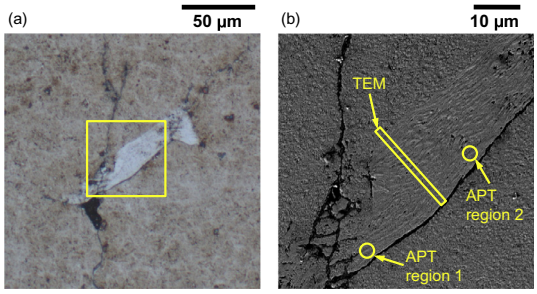

Figure 1. (a) An optical micrograph of a WEA. The secondary electron micrograph of the marked area is shown in (b) with the sample positions for TEM and APT investigations.

with residual spherical cementite of a few hundred nanometres and ⩽1 vol.% retained austenite.

During the testing, a WEA has been formed at ~200 μm under the surface adjacent to a crack without an inclusion. As indicated by its nomenclature, the WEA can be identified by optical microscope due to its white contrast (Fig. 1a). Secondary electron imaging does not often offer a clear contrast. Figure 1b shows clearly that protruding residual carbides in the WEA have been deformed, and elongated parallel to the main crack adjacent to the WEA. This flow-like morphology is also observed in butterflies [5,6]. While microcavities are formed due to plastic flow in butterflies [6], these features are not observed in this study. The WEA decorating the crack exhibits a sharp boundary with the undamaged matrix.

Site-specific TEM and APT specimens were extracted from the regions of the sample indicated in Figure 1b using focused ion beam techniques. For the preparation of the TEM sample, a FEI Helios NanoLab was employed. Firstly an ~2 μm thick Pt protective layer was deposited before the rough cutting with a 2–15 nA beam current. Then, an $\sim 20 \times 5.5 \mu m^2$-sized area was cut-out and finally thinned with 100–1000 pA beam current. A 300 kV Philips CM30 was used to investigate the microstructure. For APT analysis, areas of interest within the WEA were identified by SEM using a Zeiss NVision dual-column FIB instrument. The extraction of suitable samples from these areas was made using the lift-out procedure [15]. Briefly, a protective Pt strap (of approximate dimensions $20 \times 3 \mu m^2$) was deposited over each of the regions identified in Figure 1b, then the bar-shaped volume of material directly below the strap was isolated and removed by FIB-micromanipulator and mounted in sections on Si microtip posts. Each mounted section was finally sharpened using the Ga-beam to produce APT samples with an end-radius of ⩽50 nm. Ga damage during specimen preparation is minimised by using greatly reduced beam energy (2 kV) in the final stages of milling. Although some implantation of Ga into the specimen is unavoidable, only trace amounts were detected in the experiment and there were no significant levels of Ga ions in the vicinity of any of the analyses or images presented in this study. Moreover, since the measured Si concentrations in the two analyses presented here were 0.57 and 0.53 at.% respectively, no significant Si contamination is expected. Samples were analysed in a Local Electrode Atom Probe (LEAP) 3000HR and the data were reconstructed and analysed using IVAS software (version 3.6.0) [16].

The TEM specimen was mostly comprised of the WEA, but also included a small section of the main crack and a region of the undamaged matrix. The WEA is clearly delimited by the crack and the matrix. The WEA/matrix interface is shown in Figure 2a. On the right side in Figure 2a, it is seen that the matrix microstructure is that of a typical martensite which involves dislocations and twins. On the left side in Figure 2a, the nanocrystalline structure of the WEA is clearly observed displaying boundaries throughout. It was assumed that these corresponded to dislocation tangles; hence these features will be hereon termed dislocation cells.

The fine cellular structure can be identified due to the contrast displayed by the cell boundaries. Besides, the diffraction pattern obtained with 300 nm-diameter selected area aperture shows diffraction ring patterns corresponding to the ferrite (α) lattice (Fig. 2d). These observations imply that the orientation of the cells is random, as observed in previous studies [10,11,8,7,4]. A small portion of the $\{1\,1\,0\}_\alpha$ diffracted ring has been selected to obtain the dark field image of the cells (Fig. 2e). The cell size varies in the range of ~10–100 nm, which is similar to the ultrafine grains observed in butterflies [4–6]. Cells of different sizes are randomly distributed across the WEA, which comprises a homogenous nanocrystalline structure throughout the region. This is different from the microstructure in butterflies, where finer cells were observed nearby the inclusion [4,5]. Note that some faint diffraction spots were detected inside the $(1\,1\,0)_\alpha$ diffraction ring; these spots may correspond to iron carbide, which has a larger lattice parameter than ferrite. However, a dark field image with good contrast cannot be created from these spots due to their weak intensity.

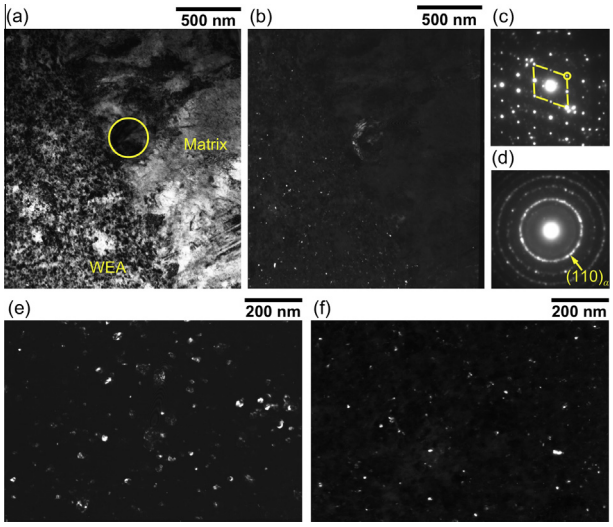

Figure 2. (a) A bright field image and (b) a cementite dark field image of the WEA/matrix interface. (c) Diffraction pattern of decaying residual carbide with the selected area aperture marked in (a). (d) A typical diffraction pattern of the nanocrystalline region. Dark field images of (e) nanocrystalline grains with the part of $(1\,1\,0)_\alpha$ diffraction ring and (f) the carbide particles with the $(1\,1\,0)_\theta$ diffraction spot in (c).